International Journal of Thermophysics, Vol. 19, No. 4, 1998

Viscous Behavior and Shear-Induced Structural Changes in Perfectly Oriented Liquid Crystals[1]

L. Bennett,[2] S. Hess,[2,3] C. Pereira Borgmeyer,[2,4] and T. Weider[2,5]

The anisotropy of the viscosity and shear-induced structural changes are studied via nonequilibrium molecular dynamics (NEMD) simulations for two types of model liquid crystals which possess both isotropic and smectic phases. These models are (a) perfectly oriented Gay–Berne particles and (b) r^{-12}-soft-spheres plus an r^{-6}-interaction with a P_2-anisotropy. Results are presented for the Miesowicz viscosity coefficients in the nematic phase. Presmectic effects are observed. Structural changes are revealed by snapshots of configurations and by the static structure factor, presented in analogy to scattering experiments. The shear-induced transition from the smectic to the nematic phase is analyzed. Similarities between magnetorheological fluids and discotic systems which can form columnar phases are discussed.

KEY WORDS: nematic liquid crystals; nonequilibrium molecular dynamics simulation; phase transition; rheology; smectic liquid crystals; structure of fluids; viscosity.

1. INTRODUCTION

The flow behavior of liquid crystals is rather complex even in the Newtonian regime of "small" shear rates. Orienting external magnetic or electric fields render the viscosity anisotropic [1–3]. In addition to the shear and bulk viscosities of simple fluids, more coefficients are needed to characterize the viscous behavior. The total number of viscosity coefficients is seven in

[1] Paper presented at the Thirteenth Symposium on Thermophysical Properties, June 22–27, 1997, Boulder, Colorado, U.S.A.

[2] Institut für Theoretische Physik, Technische Universität Berlin, Hardenbergstr. 36, D-10623 Berlin, Germany.

[3] To whom correspondence should be addressed.

[4] Present address: Telenorma GmbH, Kleyerstr. 94, D-60277 Frankfurt/M, Germany.

[5] Department of Physics, University of Colorado, Boulder, Colorado 80309, U.S.A.

0195-928X/98/0700-1143$15.00/0

the nematic phase and still larger in smectic phases. Pre- and posttransitional effects are observed in the vicinity of phase transitions, e.g., *nematic–smectic A*. Basic features of the anisotropy of the viscosity can be inferred from model fluids composed of perfectly oriented nonspherical particles. Analytical calculations and nonequilibrium molecular dynamics (NEMD) computer simulations have been performed for (prolate and oblate) ellipsoidal particles [3–5]. These special model fluids possess nematic and crystalline phases, but no smectic ones. Here results are presented for two other relatively simple types of model fluids that have nematic and smectic phases. This allows the study of pretransitional effects on the anisotropy of the viscosity of the nematic phase and the analysis of shear-induced structural changes in the vicinity of the transition to a smectic state.

After some basic remarks on the flow geometry, the viscosities of nematics, the affine transformation model, and on the simulation technique, the model potentials to be used for the present studies are introduced and results are presented. Previous MD and NEMD simulations for the viscosity of the Gay–Berne fluid in the nematic state should be mentioned [6, 7].

2. SIMULATING VISCOUS FLOW OF ANISOTROPIC LIQUIDS

2.1. Plane Couette Flow

For a simple shear flow in x-direction with the gradient in y-direction, the shear rate γ is given by $\gamma = \partial v_x/\partial y$. Such a flow can be generated either by moving boundaries or forces, or as used here, by moving image particles undergoing an ideal Couette flow with the prescribed shear rate (homogeneous shear). Such boundary conditions are known as Lees–Edwards or "sliding brick" boundary conditions, [8]. For a system in a fluid state in equilibrium, and for shear rates that are not too large, a linear velocity profile characteristic of a plane Couette flow is established. At high shear rates, where also plug-like flow occurs, it is essential to use a velocity "profile unbiased thermostat" (PUT) [9, 10]. A shear flow can also be generated by modifying the equations of motion, which leads to the so-called SLLOD algorithm (cf. Refs. 8, 11, and 12). For a recent review of NEMD results for rheological properties of simple and of complex fluids, see Ref. 13.

2.2. Pressure Tensor, Viscosity

Rheological properties such as the (non-Newtonian) viscosity and the normal pressure differences are obtained from the Cartesian components of

the stress tensor $\sigma_{\mu\nu} = -p_{\mu\nu}$ or of the pressure tensor $p_{\mu\nu}$, which is the sum of "kinetic" and "potential" contributions: $p_{\mu\nu} = p_{\mu\nu}^{\text{kin}} + p_{\mu\nu}^{\text{pot}}$,

$$Vp_{\mu\nu}^{\text{kin}} = \sum_i m_i c_\mu^i c_\nu^i, \qquad Vp_{\mu\nu}^{\text{pot}} = \tfrac{1}{2} \sum_{ij} r_\mu^{ij} F_\nu^{ij} \tag{1}$$

Here $\mathbf{c}^i$ is the peculiar velocity of particle i, i.e., its velocity relative to the flow velocity $\mathbf{v}(\mathbf{r}^i)$, $\mathbf{r}^{ij} = \mathbf{r}^i - \mathbf{r}^j$ is the relative position vector of particles i, j, and $\mathbf{F}^{ij}$ is the force acting between them. The Greek subscripts μ, ν, which assume the values 1, 2, and 3, stand for Cartesian components associated with the x, y, z-directions. In the simulations, the expression given for the pressure tensor is averaged over many (10^3 to 10^6) time steps. For the present flow geometry, the (non-Newtonian) viscosity η is obtained by dividing the yx-component (21-component) of the stress or pressure tensor by the shear rate γ: $\eta = \sigma_{yx}/\gamma = -p_{yx}/\gamma$. The kinetic contribution to the viscosity is the dominating one in dilute gases. In dense fluids (liquids), the potential contribution is the more important one.

2.3. Anisotropy of the Viscosity in Nematic Liquid Crystals

In nematic liquid crystals, the viscosity becomes anisotropic when the average orientation of the molecules is fixed by an external magnetic (or electric) field. Four such orientations are needed to determine the full anisotropy of the shear viscosity. These cases, indicated by the labels $i = 1, 2, 3, 4$ for the pertaining shear viscosities η_i, denote that the preferential orientation is held parallel to the flow velocity ($i = 1$), to its gradient ($i = 2$), to the vorticity (which is perpendicular to the preceding two directions) ($i = 3$), and to the bisector in the flow plane (xy-plane) ($i = 4$). The first three viscosities are referred to as Miesowicz coefficients, and the difference $\eta_{12} = 4\eta_4 - 2\eta_1 - 2\eta_2$ is called the Helfrich viscosity [1]. In substances like 4-methoxybenzylidene-4′-n-butyl-aniline (also called MBBA) or p-methoxy-p'-butylazoxybenzene (the mixture known as N4), which exist in the nematic state over a rather wide temperature interval, one has $\eta_2 > \eta_3 > \eta_1$. Except in the immediate vicinity of the nematic–isotropic phase transition temperature T_{NI}, where the nematic (Maier–Saupe) order parameter S varies strongly, the ratios η_2/η_3 and η_3/η_1 are practically independent of the temperature T. Thus, the computationally simpler model fluids of perfectly oriented particles (corresponding to $S = 1$) reveal many features typical for the anisotropy of the viscosity of nematic liquid crystals. In the NEMD simulation, the viscosities are obtained according to

$$\eta_i = -p_{yx}^i/\gamma \tag{2}$$

where p^i_{yx} is the yx component of the pressure tensor [cf. Eq. (1)] for the four above mentioned cases. Of course, the interaction potential must be modified appropriately in order to describe nonspherical particles. Special cases of non-spherical interaction potentials are given later. In the oriented system, the pressure tensor has an antisymmetric part, which is associated with the torque acting on the particles. This antisymmetric part is used in NEMD simulations to obtain the Leslie viscosity coefficients γ_1 and γ_2 according to

$$\gamma_1 + \gamma_2 = 2(p^1_{xy} - p^1_{yx})/\dot{\gamma}, \qquad \gamma_1 - \gamma_2 = 2(p^2_{xy} - p^2_{yx})/\dot{\gamma} \tag{3}$$

where again the superscripts 1, 2 refer to the orientations mentioned above. Due to the Onsager–Parodi relation $\gamma_2 = \eta_1 - \eta_2$, only five of the six "nematic" viscosity coefficients used so far are linearly independent. In addition to the bulk viscosity, there are two coefficients, also linked by an Onsager relation, which couple the symmetric traceless and the trace parts of the pressure and of the velocity gradient tensors. Hence, seven coefficients are needed to describe the viscous properties of nematic liquid crystals [3].

2.4. Affine Transformation Model

All coefficients, except for the bulk viscosity, have been calculated, and the Onsager–Parodi relation has been tested for model fluids of perfectly oriented ellipsoidal particles where the nonspherical interaction potential is obtained from a spherical one, e.g., a Lennard–Jones or soft spheres (SS) interaction, by an affine transformation. Both prolate and oblate ellipsoids of revolution with axis ratios $Q > 1$ and $Q < 1$, respectively, were studied [3–5]. Motivated by the success in the comparison of MD data for the anisotropy of the diffusion in model fluids having a variable degree of orientation with a modified affine transformation model [15], similar considerations have been made for the viscosity coefficients [16].

The affine transformation model states that, for perfectly oriented ellipsoidal particles with a molecular axis ratio Q, the following relationships exist [3, 4, 14]

$$Q^{-2}\eta_2^{\text{pot}} = \eta_3^{\text{pot}} = Q^2\eta_1^{\text{pot}}, \qquad \eta_{12}^{\text{pot}} = -\gamma_1 \tag{4}$$

$$\gamma_1 = (Q - Q^{-1})\,\eta_3^{\text{pot}}, \qquad \gamma_2 = (Q^{-2} - Q^2)\,\eta_3^{\text{pot}} \tag{5}$$

where the superscript "pot" denotes the contribution due to the potential. The inequalities

$$\eta_1 < \eta_3 < \eta_2, \qquad \gamma_2 < 0 \tag{6}$$

typical for nematics ($Q > 1$) are also found in the simulations. For nematic discotics ($Q < 1$) one has

$$\eta_2 < \eta_3 < \eta_1, \qquad \gamma_2 > 0 \tag{7}$$

This is also confirmed in the simulations for nematic discotics [5].

In the nematic phase, the results of the affine transformation model can be used to estimate the viscous properties of more general model fluids, such as the Gay–Berne potential. If the model potential also allows smectic phases to occur, disk-like clusters of molecules are expected to occur in the nematic phase close to the transition to the smectic one as precursors to the smectic layers. Provided that these clusters behave as oblate molecules in the nematic phase, the typical nematic order in the magnitude of the viscosity coefficients [Eq. (6)] should change to the nematic discotic order [(Eq. 7)] when the nematic–smectic transition is approached. Indications of such a behavior are seen in experiments with a substance referred to as 8CBP [2].

3. THE PERFECTLY ORIENTED GAY–BERNE FLUID

3.1. The Model

The intermolecular potential as a function of the intermolecular vector $\mathbf{r}$ and the orientation $\mathbf{n}$ for the perfectly oriented Gay–Berne (POGB) model has the following form:

$$\Phi(\mathbf{n}, \mathbf{r}) = 4\varepsilon(\mathbf{n}, \mathbf{r}) \left[\left(\frac{\sigma_0}{r - \sigma(\mathbf{n}, \mathbf{r}) + \sigma_0} \right)^{12} - \left(\frac{\sigma_0}{r - \sigma(\mathbf{n}, \mathbf{r}) + \sigma_0} \right)^{6} \right] \tag{8}$$

where the shape parameter, $\sigma(\mathbf{n}, \mathbf{r})$, is given by

$$\sigma(\mathbf{n}, \mathbf{r}) = \sigma_0 \left(1 - \chi' \left\{ \frac{(\mathbf{r} \cdot \mathbf{n})^2}{r^2[1 + \chi']} \right\} \right)^{-1/2} \tag{9}$$

and the interaction strength, $\varepsilon(\mathbf{n}, \mathbf{r})$, by

$$\varepsilon(\mathbf{n}, \mathbf{r}) = \varepsilon_0 \varepsilon_1{}^{\nu} \varepsilon_2{}^{\mu}(\mathbf{n}, \mathbf{r}), \qquad \varepsilon_1 = [1 - \chi^2]^{-1/2}, \qquad \varepsilon_2(\mathbf{n}, \mathbf{r}) = 1 - \chi' \left\{ \frac{(\mathbf{r} \cdot \mathbf{n})^2}{r^2[1 + \chi']} \right\} \tag{10}$$

Here ε_0 and σ_0 are the characteristic energy and molecular diameter of the Lennard–Jones potential. The parameter χ depends on the ratio

$\kappa = \sigma_{ee}/\sigma_{ss}$, where σ_{ee} is the length of the molecule and σ_{ss} the width. The parameter χ' depends on the ratio $\kappa' = \varepsilon_{ee}/\varepsilon_{ss}$, where ε_{ee} and ε_{ss} are the minima of the potential for the end–end and side–side configurations, respectively. The values of the various parameters used were $\mu = 2$, $\nu = 1$, $\kappa = 3$, and $\kappa' = 5$.

The potential was cut off and shifted at $r = 4\sigma$ in order to remove the discontinuity. The simulations were performed using 256 particles in a cubic box with Lees–Edwards boundary conditions and a simple velocity scaling thermostat. A Verlet velocity algorithm was used to solve the equations of motion. Simulations for larger systems are in progress.

3.2. Phases and Local Order

In addition to the nematic phase, which also occurs if the molecules are free to rotate, the perfectly oriented Gay–Berne fluid exhibits two equilibrium phases not seen in simulations of the full Gay–Berne model [17]: SmA and a SmB "quadratic," a layered phase with short-range four-fold order within the layers (Fig. 1). The nematic and the smectic states were subjected to a shear flow. A tilted SmB hexatic phase also occurs. The SmB

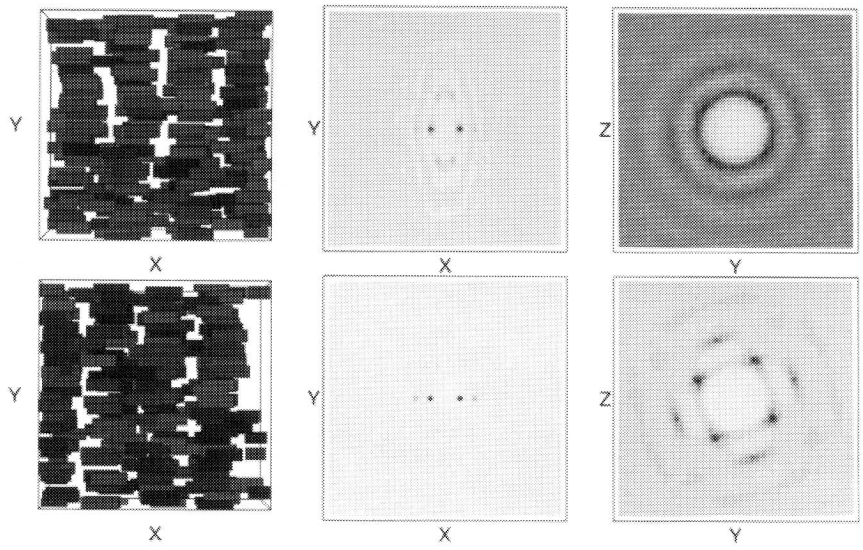

Fig. 1. $T = 1.00$: A snapshot and static structure factors for the xy and yz planes. Top, $\rho = 0.28$, SmA; bottom, $\rho = 0.29$, four-fold order within layers (densities in reduced units).

"quadratic" phase is found to be metastable: in the case where the orientation is parallel to the velocity gradient, low shear rates result in a tilting of the layers with respect to the director together with a change in symmetry within the layers. The resulting tilted SmB hexatic phase remains stable after the shear is removed.

3.3. Viscosities

Miesowicz viscosities have been obtained for the nematic and presmectic regions (Fig. 2). The lowest viscosity is that for the orientation parallel to the shear velocity, η_1, the largest occurring for the orientation parallel to the velocity gradient, η_2, as the affine transformation model predicts. However, the expected reordering of the Miesowicz coefficients from $\eta_2 < \eta_3 < \eta_1$ in the nematic phase to $\eta_1 < \eta_3 < \eta_2$ in the smectic A phase is not observed due to the shear-induced tilt transition for small shear rates (Fig. 3). One can observe, however, that for a density $\rho = 0.29$ and a shear rate $\gamma = 0.02$ (in standard reduced units; cf. Ref. 8, Appendix B) the viscosity for the orientation parallel to the shear velocity approaches that for the orientation perpendicular to both the shear velocity and its

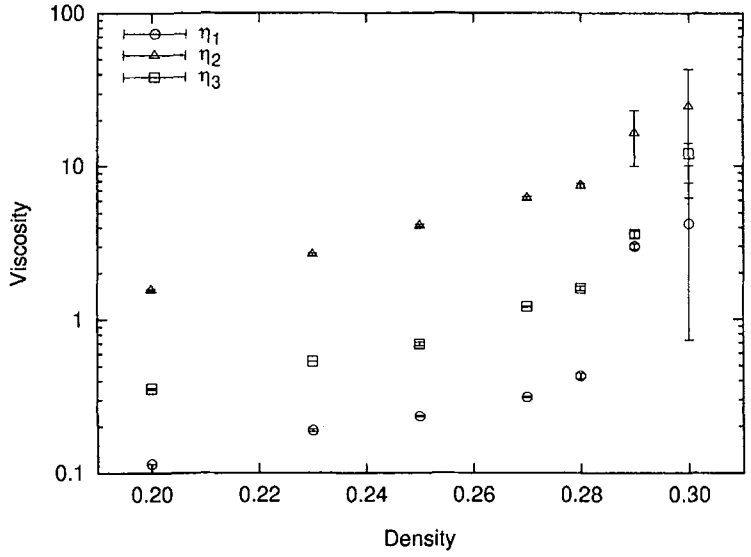

Fig. 2. The Miesowicz viscosities as a function of density for $T = 1.00$, obtained by extrapolating the shear rate to zero.

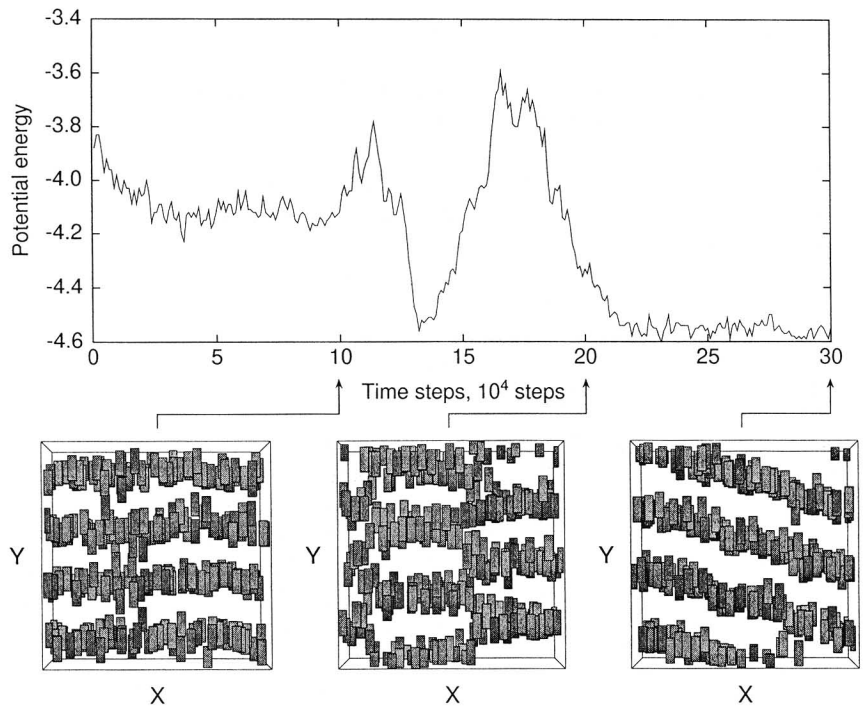

Fig. 3. State point $T = 1.00$, $\rho = 0.300$. After 10^5 time steps, a shear rate of 0.01 is applied. The shear is switched off after a further 10^5 time steps and the system allowed to relax for yet another 10^5 time steps.

gradient. The Leslie coefficient γ_1 remains smaller than the absolute magnitude of the Leslie coefficient γ_2 for both the nematic and the smectic region, and in accordance with the affine transformation model. As expected, γ_2 is negative throughout.

According to the affine transformation model, the ratios $R_{31} := \sqrt{\eta_3/\eta_1}/Q$ and $R_{23} := \sqrt{\eta_2/\eta_3}/Q$ both are equal to 1. The NEMD simulations for LJ ellipsoids yielded $R_{31} = 0.80$ and $R_{23} = 0.91$ [4]. Typical experimental values, e.g., for MBBA at 30°C, are $R_{31} = 0.52$ and $R_{23} = 0.71$. For the present model one finds, in the density range $0.20 \leqslant \rho \leqslant 0.28$, the values $0.56 \leqslant R_{31} \leqslant 0.66$ and $0.70 \leqslant R_{23} \leqslant 0.81$. Thus, if one compares the predictions of the affine transform model with NEMD and experimental results, one finds the agreement between the POGB model and experiment is rather good, particularly for lower densities. Whereas the perfect orientation tends to lead to an increase in the effective molecular axis ratio Q, the well-depth anisotropy causes a decrease in the effective Q.

4. ANISOTROPIC SOFT SPHERES

In analogy to the ferrofluids and magnetorheological fluids to be discussed in the next section, a relatively simple model was introduced [13] for liquid crystals where a transition from the nematic to the smectic A phase is possible. A further smectic phase (smB) also occurs, in addition to the solid state. The potential comprises a r^{-12} soft spheres term and an extra anisotropic interaction with a symmetry given by the second Legendre polynomial, $P_2 = \frac{3}{2}(r^{-2}(\mathbf{r}\cdot\mathbf{n})^2 - \frac{1}{3})$, the strength of which is determined by the parameter Φ_{anis}:

$$\Phi = \varepsilon_0 \left(\frac{\sigma_0}{r}\right)^{12} + \Phi_{\text{anis}} \left(\frac{\sigma_0}{r}\right)^{6} \left(r^{-2}(\mathbf{r}\cdot\mathbf{n})^2 - \frac{1}{3}\right) \tag{11}$$

Again, the unit vector $\mathbf{n}$ (director) specifies the preferential direction. For $\Phi_{\text{anis}} > 0$ this potential models elongated (prolate) particles. At the state point $T = 0.25$, $\rho = 0.6$, in SS units, and with the interaction cutoff at $r = 2.5\sigma_0$, the transition nematic–smectic A occurs at $\Phi_{\text{anis}} \approx 2.3$ (in units of ε_0). The director $\mathbf{n}$ can be chosen parallel to the directions discussed above in connection with the anisotropy of the viscosity. The resulting Miesowicz viscosities η_1, η_2, η_3 show surprisingly complex behavior as functions of the anisotropy parameter Φ_{anis} at shear rates which are, at least for the nematic phase, in the Newtonian flow regime [13]. The typical nematic order [Eq. (6)] in the magnitude of the viscosities is found for $0 < \Phi_{\text{anis}} < 1$. For $1 < \Phi_{\text{anis}} < 2.3$, presmectic effects change this behavior. In the smectic phase, for $\Phi_{\text{anis}} > 2.8$, the order of the viscosities corresponds to that of a nematic discotic system [Eq. (7)]. The shear flow breaks the smectic layers, but disk-like correlated clusters remain. The shear-induced structural changes have been analyzed. The scenario of the crossing of the viscosity coefficients is even more complex than in experiments with 8CBP, where η_1 becomes larger than η_3, but does not quite reach η_2 when the temperature is lowered toward the nematic–smectic transition [2].

4.1. Magnetorheological Fluids

For $\Phi_{\text{anis}} < 0$, the potential function [Eq. (11)] models nematic discotic substances where a transition from the nematic to a columnar phase occurs with increasing magnitude of the nonsphericity parameter. Qualitatively, this behavior is quite similar to that of magnetorheological (MR) fluids [or electro-rheological (ER) fluids] in the presence of an applied magnetic (or electric) field. Ferro-fluids and MR fluids have been modeled by soft spheres plus a dipole–dipole interaction [18]. This corresponds to the

potential [Eq. (11)] with the r^{-6} factor of the term $(r^{-2}(\mathbf{r}\cdot\mathbf{n})^2-\frac{1}{3})$ replaced by $-\varepsilon_{\text{mag}}(\sigma_0/r)^3$. Here, the parameter $\varepsilon_{\text{mag}}>0$ is proportional to the square of the (induced) magnetic moment of the particles which are parallel to $\mathbf{n}$. Pairs of such particles feel a disk-like interaction since, for fixed relative kinetic energy, they can approach each other more closely in the direction parallel to $\mathbf{n}$ than in the perpendicular directions. Thus it is not surprising that ferrofluids show an anisotropy of the viscosity analogous to nematic discotic liquid crystals [3, 5]. When the dipole–dipole interaction is stronger, however, chains are formed which, at higher densities, are arranged in partially ordered spatial structures. This affects the viscous behavior in a dramatic way [13]. In the simulations, the interaction was again cut off (smoothly) at $r=2.5r_0$, and $N=1000$ particles were used. At the state point $T=0.25$, $\rho=0.6$, in SS units and for the shear rate $\gamma=0.06$, e.g., one finds the discotic behavior $\eta_1>\eta_2$ for $0<\varepsilon_{\text{mag}}<3$. For $\varepsilon_{\text{mag}}>3$, the viscosity η_2 for the field parallel to the gradient direction increases by more than one order of magnitude when ε_{mag} is increased from 2 to 6. A yield stress occurs for the higher values of the dipole–dipole interaction. This is typical for the MR fluids which are similar to the ferro-fluids but which are composed of particles with stronger dipole–dipole interaction and usually contain a higher volume fraction of colloidal particles.

5. CONCLUSION

The perfectly oriented Gay–Berne potential and anisotropic soft spheres have been used to study the viscous and structural properties of model fluids in the vicinity of the nematic–smectic phase transition. Further simulations for freely orienting particles are desirable, so that phenomena in the vicinity of the isotropic–nematic and isotropic–smectic transitions can also be analyzed. For model fluids of short chain molecules with a stiff central part and flexible ends which possess a broad smectic A phase [22], studies of rheological properties and of the shear-induced structural changes are in progress.

ACKNOWLEDGMENTS

Financial support provided by the Deutsche Forschungsgemeinschaft (DFG) via the Sonderforschungsbereich 335 "Anisotrope Fluide," as well as the generous donation of computer time by the Konrad-Zuse-Zentrum für Informationstechnik (Berlin) and by the Höchstleistungsrechenzentrum der Kfa Jülich GmbH, are gratefully acknowledged.

REFERENCES

1. P. G. de Gennes, *The Physics of Liquid Crystals* (Clarendon Press, Oxford, 1974); Chap. 3. H. Kelker and R. Hatz, *Handbook of Liquid Crystals* (Verlag Chemie, Weinheim, 1980). G. Vertogen and W. de Jeu, *Thermotropic Liquid Crystals, Fundamentals* (Springer, Berlin, 1988).
2. H. Kneppe, F. Schneider, and N. K. Sharma, *Ber. Bunsenges Phys. Chem.* **85**:784 (1981). H. Kneppe and F. Schneider, *Mol. Cryst. Liq. Cryst.* **65**:23 (1981). H.-H. Graef, H. Kneppe, and F. Schneider, *Mol. Phys.* **77**:521 (1992).
3. S. Hess, *J. Non-Equil. Thermodyn.* **11**:176 (1986).
4. D. Baalss and S. Hess, *Phys. Rev. Lett.* **57**:86 (1986); *Z. Naturforsch.* **43a**:662 (1988).
5. H. Sollich, D. Baalss, and S. Hess, *Mol. Cryst. Liq. Cryst.* **168**:189 (1989). J. Schwarzl and D. Baalss, *J. Phys. Condens. Matter* **2**:SA279 (1990).
6. A. M. Smondyrev, G. B. Loriot, and R. A. Pelcovits, *Phys. Rev. Lett.* **75**:2340 (1995).
7. S. Sarman and D. J. Evans, *J. Chem. Phys.* **99**:9021 (1993).
8. M. P. Allen and D. J. Tildesley, *Computer Simulation of Liquids* (Clarendon, Oxford, 1987).
9. D. J. Evans and W. G. Hoover, *Annu. Rev. Fluid Mech.* **18**:243 (1986).
10. W. Loose and S. Hess, *Rheol. Acta* **28**:91 (1989). S. Hess and W. Loose, *Physica A* **162**:138 (1989); *Ber. Bunsenges. Phys. Chem.* **94**:216 (1990).
11. W. G. Hoover, *Molecular Dynamics* (Springer, Berlin, 1986); *Computational Statistical Mechanics* (Elsevier, Amsterdam, 1991).
12. D. J. Evans and G. P. Morris, *Statistical Mechanics of Nonequilibrium Liquids* (Academic Press, London, 1990).
13. S. Hess, M. Kröger, W. Loose, C. Pereira Borgmeyer, R. Schramek, H. Voigt, and T. Weider, *Monte Carlo and Molecular Dynamics of Condensed Matter Systems*, K. Binder and G. Ciccotti, eds. (IPS Conf. Proc. **49**, Bologna, 1996), pp. 825–841; S. Hess, *Computational Physics*, K. H. Hoffmann and M. Schreiber, eds. (Springer, Berlin, 1996), pp. 268–293.
14. W. Helfrich, *J. Chem. Phys.* **50**:100 (1969); **53**:2267 (1970).
15. S. Hess, D. Frenkel, and M. P. Allen, *Mol. Phys.* **74**:765 (1991).
16. H. Ehrentraut and S. Hess, *Phys. Rev. E* **51**:2203 (1995).
17. E. de Miguel, L. F. Rull, M. K. Chalam, and K. E. Gubbins, *Mol. Phys.* **74**:405 (1991).
18. S. Hess, J. B. Hayter, and R. Pynn, *Mol. Phys.* **53**:1527 (1984).
19. F. Affouard, M. Kröger, and S. Hess, *Phys. Rev. E* **54**:5178 (1996).